Numerical Estimates of Humidity in a Membrane-Filter Ice Nucleus Chamber

G. GARLAND LALA AND JAMES E. JIUSTO[1]

Dept. of Atmospheric Science, State University of New York at Albany 12203

(Manuscript received 18 November 1971, in revised form 25 February 1972)

ABSTRACT

A one-dimensional model was developed to examine humidity fields within a conditioning chamber for measuring ice nucleus concentrations on millipore filters. Representative concentrations of ice and cloud condensation nuclei were assumed, and the interplay among these growing particles (vapor sinks), the supply flux of vapor, and the resultant relative humidity at and above the filter surface investigated.

The model suggests that water saturation is not achieved under typical operating conditions of such chambers. Maximum humidities reached decrease with increasing numbers of either condensation or ice nuclei, thereby offering another possible explanation of the filter volume effect. Most favorable operating conditions for achieving highest chamber humidities are delineated. The results suggest that this technique is capable of detecting mixed condensation-freezing nuclei, deposition nuclei and some contact nuclei, with the former perhaps being most common not only in filter measurements but also in the atmosphere.

1. Introduction

No entirely satisfactory method of measuring the concentration of ice nuclei in ambient air has yet been devised. The principal techniques being employed today involve expansion chambers, mixing or diffusion chambers (with optical or acoustic sensing of crystals), bulk droplet freezing, and membrane or millipore filter (MF) processing. As reported at the Second International Workshop on Condensation and Ice Nuclei (Weickmann and Podzimek, 1971), considerable disparity in ice nucleus concentration measurements occurs with varying apparatus.

The millipore filter technique, as first devised by Bigg *et al.* (1963) and then substantially improved by Stevenson (1968), is being fairly extensively used. One example was the cooperative MF sampling experiment conducted at 44 sites around the globe from January to April 1969 (Bigg and Stevenson, 1970). Despite the so-called volume-effect problem, wherein ice nucleus concentrations are observed by some investigators to decrease with increasing sampled volume, presumed advantages of the MF method include its potential for large-volume sampling, long activation time of nuclei, and precise control of relative humidity in the filter conditioning chamber.

The latter device is in essence a thermal gradient diffusion chamber in which water vapor molecules diffuse from an upper ice surface to a lower colder surface holding the filter and its nuclei. Generally one selects a temperature differential that will just produce water saturation at the filter surface so as to expose the nuclei to representative cloud conditions. Some investigators, e.g., Gagin and Aroyo (1969), also operate over a range of relative humidities from subsaturation to supersaturation with respect to water.

In order for any diffusion chamber to reach and maintain prescribed humidities, it is essential that the supply flux of water vapor considerably exceed depletion by wall surfaces and the activated nuclei (ice and condensation). It was not apparent from the literature that vapor source vs sink calculations had been performed for "ice chambers," as had been done previously for cloud condensation nuclei chambers (Twomey, 1959). Rather, one can only assume from stated temperature differentials and corresponding humidities that vapor losses by nuclei were ignored or considered negligible. The latter did not appear realistic, recognizing the high concentrations of 0.1 μ or larger particles typically captured by a filter ($\sim 10^7$–10^8 cm^{-2}). Consequently, a numerical time-dependent model of chamber conditions was undertaken to examine: 1) actual filter-surface relative humidity for representative ice and condensation nucleus concentrations; 2) a quantitative assessment of the sample volume effect; and 3) optimum methods of operating such chambers or modified versions thereof.

2. Mathematical formulation

The physical basis for this model is that the rate of removal of water vapor by growing droplets and ice crystals is controlled by the diffusive flux of source water vapor, which determines the relative humidity over the filter. The chamber was assumed to consist of

[1] Also Atmospheric Sciences Research Center.

two parallel surfaces separated by a distance h. The upper surface at height z_0 is a uniform layer of ice and the lower surface at z_h is a dry support for the filter. Computations of the vapor concentration ρ, at various levels z in the chamber, are based on the diffusion equation

$$\frac{\partial \rho}{\partial t}=\frac{\partial^2 \rho}{\partial z^2}, \tag{1}$$

where D is the diffusivity of water vapor. (All symbols are defined in Appendix A.) Under the assumption of a horizontally homogeneous field with reasonably small vertical gradients of temperature and vapor concentration, this equation is appropriate.

The low concentrations of ice nuclei typically occurring in the atmosphere require that large volumes of air be sampled with a millipore filter. Along with the ice nuclei, an enormous number of other small particles are collected, of which the hygroscopic or mixed particles have the most important influence on the humidity in the conditioning chamber. These soluble particles form droplets of solution at humidities below water saturation whose equilibrium sizes increase with increasing humidity. We have assumed an initial dry size range for these soluble particles of 0.1 to 1.0 μ, distributed according to the Junge law (inverse size cubed). These particles, covering the so-called cloud nucleus size range,[2] were assumed to be composed of sodium chloride.

For the larger of these particle sizes ($>0.6\,\mu$ radius) and for humidities $>98\%$, the well-known droplet growth equation of Fletcher (1966) was used, i.e.,

$$\frac{dr}{dt}=\frac{G}{r}\left(S-1-\frac{a}{r}+\frac{b}{r_3}\right)=\frac{G}{r}(S-S'), \tag{2}$$

where r is the drop radius, G a thermodynamic factor, a and b the curvature and solution terms, and S the saturation ratio. At lower humidities and with smaller particle sizes, this equation becomes difficult to use accurately because the sum of the terms inside the parentheses is very small. Physically, this is an indication that the particles are close to the equilibrium size during this stage of their growth. Because of this near-equilibrium condition, we were able to assume that the magnitude and time derivative of the saturation ratio over the drop were equal to the environmental values ($S\approx S'$, $dS/dt\approx dS'/dt$). Under this assumption a new drop equation is formed wherein the droplet is always in equilibrium with the varying ambient saturation ratio. Hence, the equation for droplet growth is

$$\frac{dr}{dt}=\frac{dr}{dS'}\frac{dS}{dt}=\frac{r^4}{3b-ar^2}\frac{dS}{dt}. \tag{3}$$

Trial machine computations, carried out in double precision, indicated excellent agreement between Eqs. (2) and (3) for small nuclei at low humidities.

Ice nuclei seemingly present greater difficulties than the condensation nuclei due to the lack of agreement on their size and activation properties. Fortunately, the final size of an ice crystal is almost independent of the nucleus size due to rapid initial growth. The importance of nucleus size is further reduced because the low concentration of ice nuclei (IN) relative to cloud condensation nuclei (CCN) in the sample, typically 10^{-5}–10^{-6} IN/CCN, requires relatively large crystals before the ice phase can compete effectively with the droplets in the vapor depletion process. The sizes of the ice nuclei were assumed to be uniformly small (0.05 μ radius) for all particles. The activation behavior of ice nuclei under variable conditions is not well understood and is, in fact, one of the relationships that one would hope to study with the millipore filter technique. To circumvent this difficulty and still maintain reasonable correspondence to observations, a crystal concentration equation dependent on time, similar to that of Alkazweeny (1970), was used, i.e.,

$$n=N_0(1-e^{-t/\tau'}), \tag{4}$$

where n is the number of crystals, N_0 the number of crystals after 20 min, and τ' the time constant (typically 6 min). This equation has been discussed by Fletcher (1959) as giving a good representation of the time dependence of the ice crystal count in mixing chambers, as well as possessing theoretical merit. Subsequently, sample computations were repeated with ice crystal activation dependent upon humidity rather than time. The results were very similar indicating that the results are primarily dependent on the rapid formation of ice crystals early in the development process. It was further assumed that the continuous function (4) can be approximated by ten discrete values, each differing from the other by $0.1N_0$. Due to the nature of the function (4), each fractional increase in concentration is separated from the previous value by an increasing time interval or activation time. (Analogously, five droplet size categories proved sufficient.)

The sizes of the crystals were calculated from the standard mass diffusion equation

$$\frac{dm}{dt}=4\pi G'C(\rho/\rho_{s1}-1), \tag{5}$$

where the crystal capacitance factor

$$C=\begin{cases} r_c \text{ (sphere)} \\ \dfrac{2r_c}{\pi} \text{ (plate)} \end{cases}$$

G' is a thermodynamic factor, and r_c is crystal radius. While (5) applies to a crystal in free space and not

[2] The exclusion of smaller Aitken nuclei does not significantly alter the calculations owing to the relatively modest mass of water absorbed by these particles.

precisely to one resting on a porous filter, the effect on the ambient humidity field is considered minor.

The initial shape of the crystal was assumed to be spherical with a transition to plate type growth at 4.5 μ where the planar radius growth rate commences to exceed the spherical crystal growth rate. The mass-size relationship of plate crystals was taken as

$$m=3.04\times10^{-3}r^2$$

based on prior work (Nakaya, 1954; Jiusto *et al.*, 1970).

The vapor depletion in grams per square centimeter of filter caused by the growing crystals and droplets is given by the sum over all size ranges of the product of the surface concentration σ and mass growth rate of the particles:

$$\sum_i \sigma_{i1}\frac{dm_{i1}}{dt}+\sum_{j=0}^{j=k(t)}\sigma_{j2}\frac{dm_{j2}}{dt}, \tag{6}$$

where the subscripts 1 and 2 refer to the droplets and ice crystals, respectively. The limits on the second summation are expressed as a function of time to indicate the activation of additional classes of crystals according to Eq. (4).

Possible effects on the humidity due to the adsorption of water vapor or to condensation on the filter fibers have been neglected. At high humidities near water saturation one would expect some adsorption to occur, but the uncertain magnitude of the effect is considered relatively small. Should water saturation be achieved or exceeded, filter condensation could be significant.

The initial state of the chamber is one of uniform temperature and vapor concentration. It is realistically assumed that the temperature throughout the chamber is the temperature of the top plate and the vapor concentration is the ice saturation value at the top plate temperature. The lower surface, including the filter, is also assumed initially to be at these conditions.

The driving force to increase humidity at the filter is provided by cooling of the bottom plate. The temperature T of the lower surface will decrease exponentially as heat is pumped out by the customarily employed thermo-electric cooler. Hence,

$$T=T_f-(T_0-T_f)e^{-(t/\tau)}, \tag{7}$$

where T_0 and T_f are the initial and final temperatures and τ is the time constant (which for some apparatus is on the order of 1 min).

The decrease of temperature at the lower surface reduces the ice and water saturation vapor concentration. For ease of computation, the saturation vapor concentrations of each water phase ρ_{si} were computed from the well-known Magnus approximation given by

$$\rho_{si}=e_0R_v^{-1}T^{-1}10^{[a_it'/(b_i+t')]}. \tag{8}$$

For each case the constants in this equation (a_i, b_i) are calculated from the saturation vapor concentration (determined from the Goff-Gratch formula) at the top and bottom chamber temperatures.

The boundary conditions at the chamber top ($z=0$) are given by

$$T(0,t)=T_0,$$
$$\rho(0,t)=\rho_{s2}(T_0),$$

while the initial conditions beneath the top ice surface are

$$T(z,0)=T_0,$$
$$\rho(z,0)=\rho_{s2}(T_0).$$

At the lower, colder boundary ($z=h$), the diffusive flux of vapor is equal to the vapor consumption by the particles as given previously by Eq. (6).

Eqs. (1), (3)–(8) along with the initial size of the particles and the initial and boundary conditions of the vapor field determine the solution for the relative humidity over the filter. This set of equations was solved numerically on a Univac 1108 computer. The difference approximations for the vapor diffusion, drop growth, and crystal growth equations yield implicit equations for the vapor concentration at various levels in the chamber and the particle sizes at each time step. For a chamber of 1 cm height with the vapor concentration to be determined at 10 levels, a time step of 0.05 sec proved necessary; this resulted in a real-to-machine time ratio of 5. (Details of the difference approximations and the iterative method of solution appear in Appendix B. An analytical solution would be exceedingly formidable and necessitate a number of simplifying assumptions.)

3. Results

a. Instrument behavior

The equations were solved for a number of cases representing various concentrations of ice nuclei and cloud condensation nuclei and for several sample volumes. The results apply to other concentrations and volumes which result in the same surface concentration of particles. The effects of chamber height, operating conditions, and the rate of cooling of the filter were also investigated.

A test of the one-dimensional (vertical) assumption as a function of chamber diameter was provided by a steady-state solution to the three-dimensional problem for a cylindrical chamber. For chamber diameters from two to five times the filter diameter, there is excellent agreement with the one-dimensional model at the center of the filter. As would be expected, the humidity at the edge of the filter was higher than in the center, but only by 0.02%. Horizontal gradients of vapor concentrations over the filter at all levels were small indicating that the one-dimensional model provides an adequate description of the processes over the filter.

For the purpose of comparison, the representative case of a 100 liter sample with 100 cloud condensation

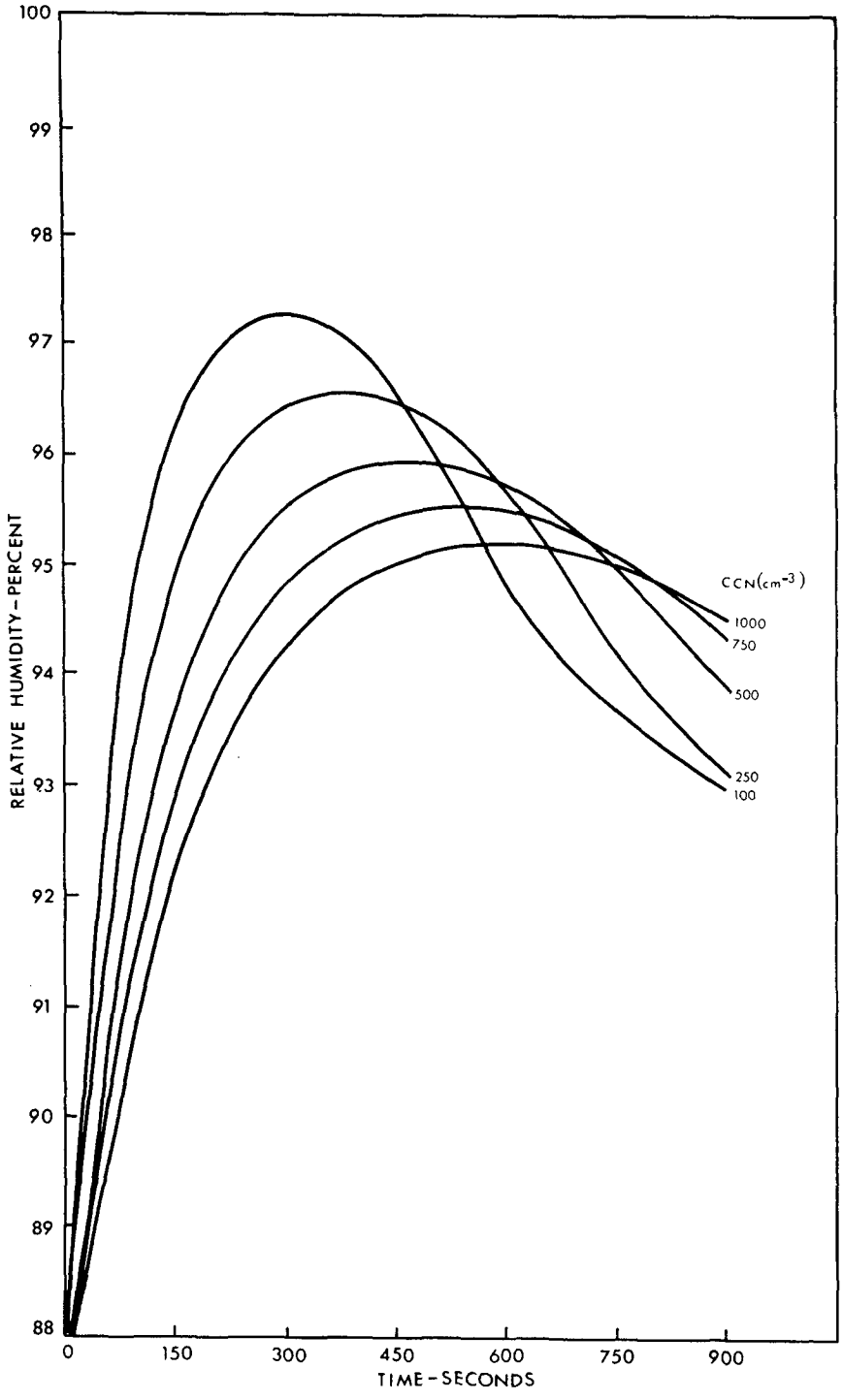

FIG. 1. Filter relative humidity vs time and varying cloud condensation nucleus concentrations (fixed ice nucleus concentration of 1 liter^{-1} and a sample volume of 100 liters).

nuclei cm^{-3} and 1.0 ice nucleus liter^{-1} and a humidity over water of "100%" (calculated under the assumption of no vapor sinks, i.e., $T_0 = -13.34$C, $T_{\text{filter}} = -15$C) was chosen as a reference. The chamber height was taken as 1 cm and the time constant for achieving the lower surface temperature of -15C was 60 sec. The humidity at the filter surface as a function of time is given in Fig. 1 by the curve labeled 100. Note that the peak humidity is 97.3%, significantly less than the value of 100% calculated without accounting for vapor

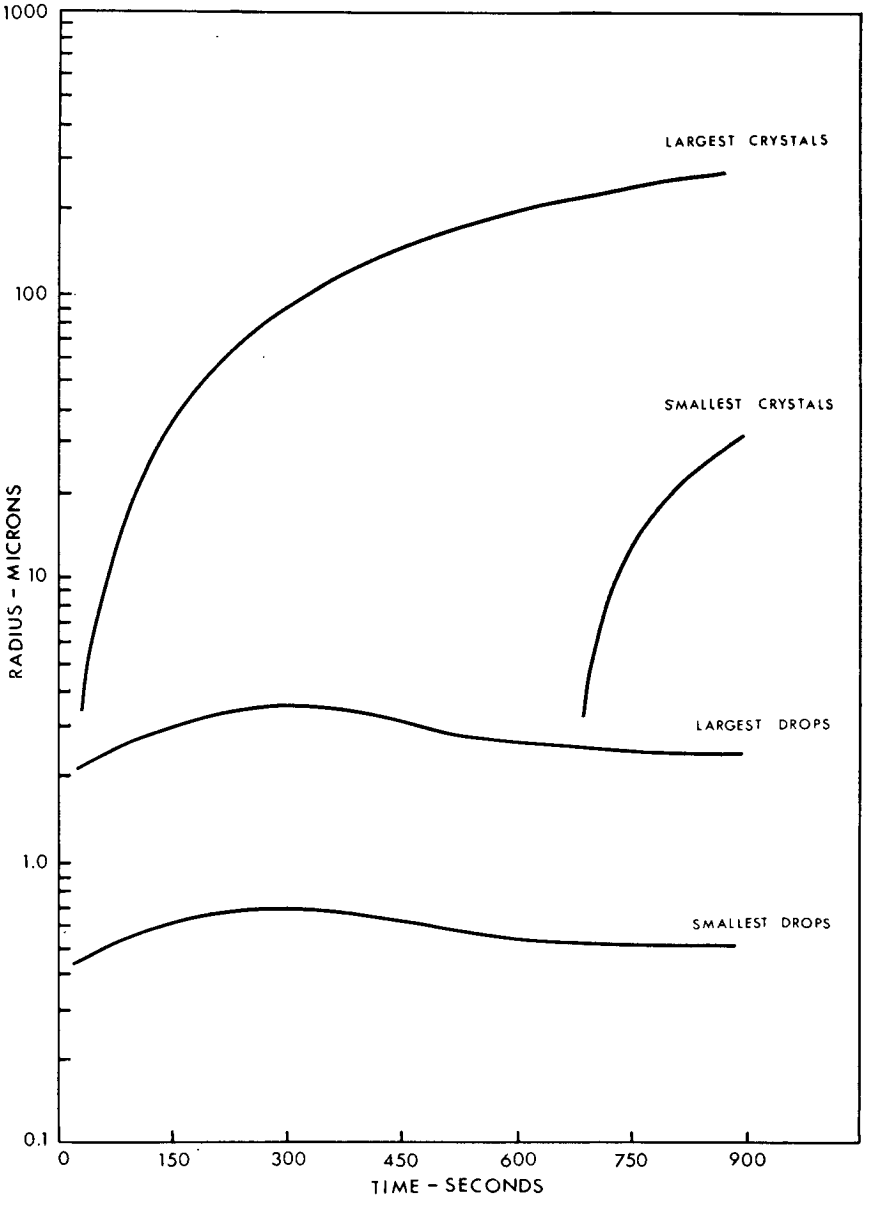

FIG. 2. Sizes of growing ice crystals and droplets for reference case (CCN = 100 cm^{-3}, IN = 1 $liter^{-1}$, volume = 100 liters).

depletion by the growing particles. The corresponding sizes of the largest and the smallest droplets and of ice crystals as a function of time are shown in Fig. 2. Extending the time to 30 min resulted in crystal sizes of 249 to 908 μ diameter, sizes which compare favorably with those measured and kindly provided by Dr. Abraham Gagin (Hebrew University, Israel).

From the humidity curve and the particle size curves, the interaction of the sinks with the supply flux of vapor can be ascertained. During the initial period, the region of rising humidity, the saturation vapor concentration at the filter is decreasing more rapidly than the ambient value. The solution droplets are the major sinks because the ice crystals are small and few in number. At the peak of the humidity curve, the rate of vapor consumption by the ice crystals is equal to the supply by diffusion. On the decreasing side of the curve, the ice crystals consume vapor at an increasing rate, forcing the humidity downward and causing droplets to evaporate. At longer times, when the droplets have become quite small, the flux of vapor is equal to the rate of consumption by the ice crystals. In the limit with large numbers of crystals, the filter humidity would approach ice saturation at the prevailing temperature.

Fig. 1 shows the variation of filter surface humidity with time for several concentrations of CCN, while

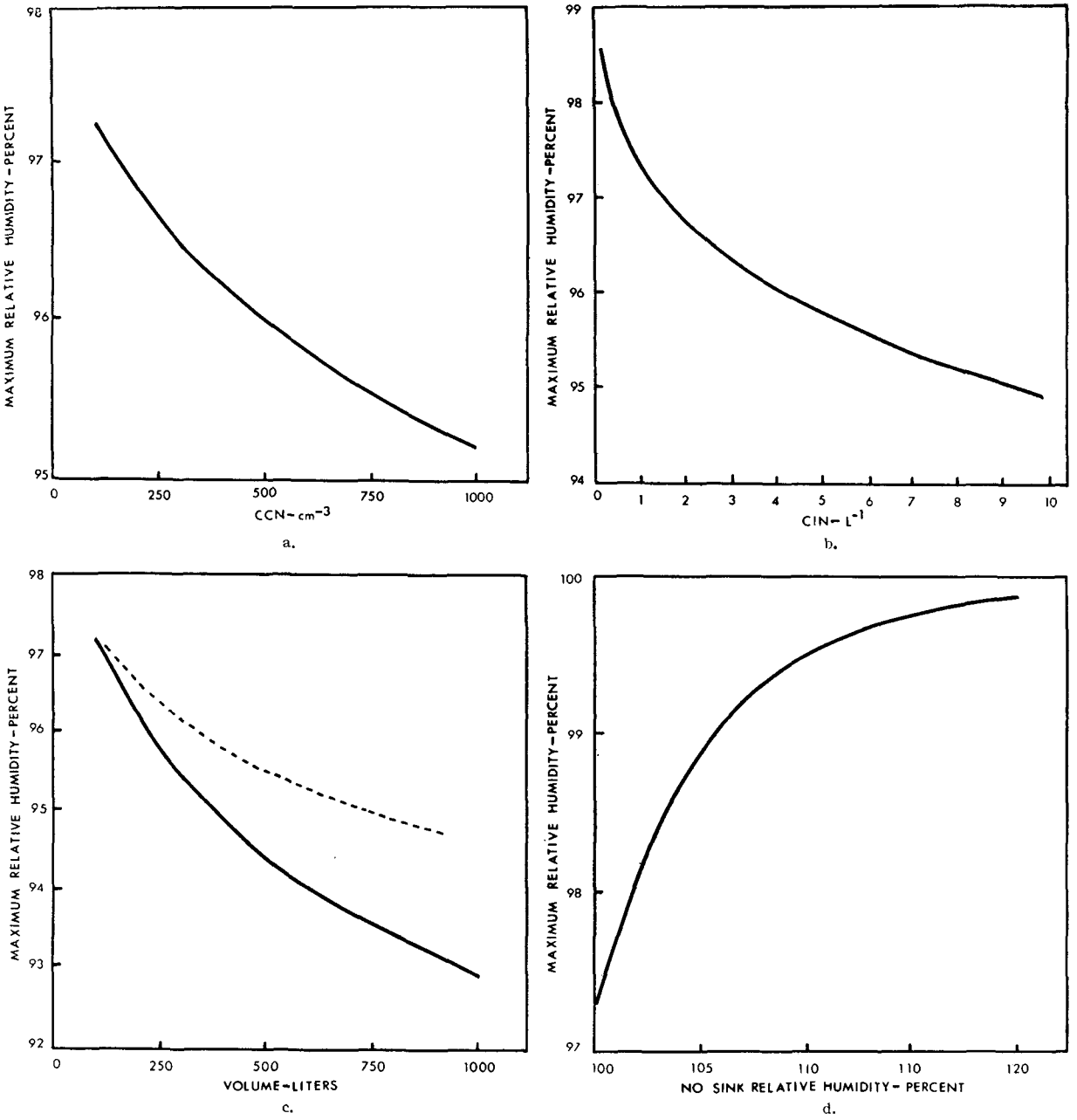

FIG. 3. Maximum fiber relative humidity as a function of CCN (a), IN (b), sample volume (c), and no-sink relative humidity (d)

Fig. 3a depicts the progressive drop in peak humidity. The effect of increasing the CCN is a slower rate of rise of the humidity which enable the ice crystals to become dominant at lower peak humidities. The broadening of the curves is due to the larger numbers of water droplets which must be "consumed" by the ice crystals in the process of decreasing the humidity.

The reference case was next altered by changing only the concentration of IN to study their effect on humidity. Fig. 3b indicates that the peak relative humidity also falls with increasing IN concentrations. The humidity as a function of time and IN concentration (Fig. 4) shows a narrowing of the curve with a rapid fall-off of humidity past the peak. In contrast to Fig. 1 (CCN variable), the curves narrow with increasing concentrations of ice nuclei because they can more quickly accommodate the vapor from the evaporating droplets.

The effect of the sample volume was investigated by taking the reference case (CCN = 100 cm^{-3}, IN = 1 $liter^{-1}$) and increasing the concentrations of CCN and IN in proportion to the volume. Fig. 3c (solid curve)

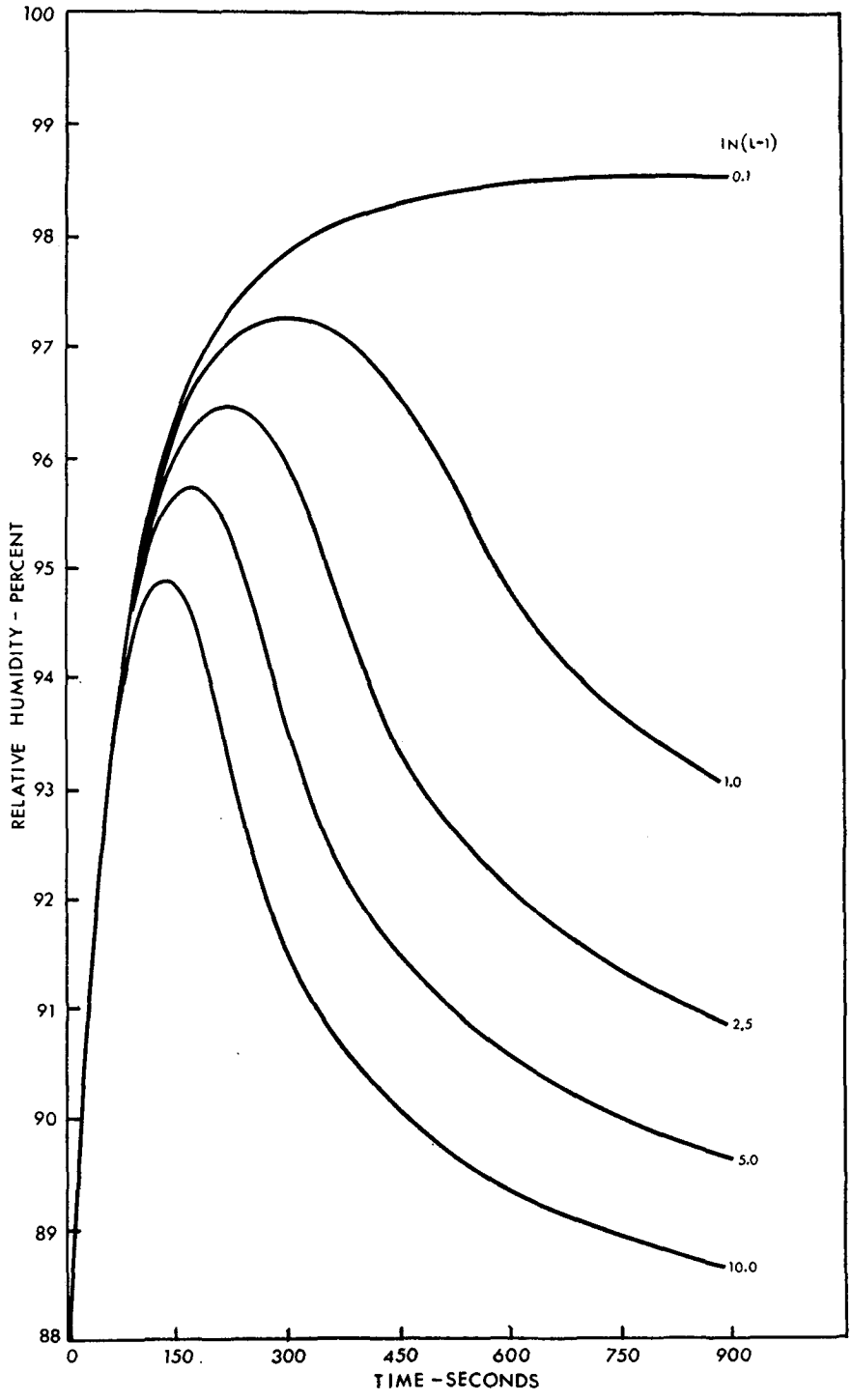

FIG. 4. Filter relative humidity vs time and varying ice nucleus concentrations (100-liter sample and fixed cloud condensation nucleus concentration of 100 cm^{-3}).

shows the decrease in the peak humidity with increased sample volume, while the general shape of the humidity-time curves vs sample volume (not shown) resembles that of Fig. 1 (100 CCN curve).

Due to the volume effect the concentration of IN does not increase in proportion to the volume. To obtain results pertinent to actual observations, several cases were computed for which the IN concentrations were based on observed relative concentration as a function of volume. The measured data used were those

of Gagin and Aroyo (1969)—their Fig. 2 average IN concentration curve. The concentration of CCN was maintained proportional to the volume. The peak humidity achieved for these cases is indicated by the dashed curve in Fig. 3c. Even with the reduced numbers of ice crystals, the decrease in the peak humidity is still very significant.

As sample volume increases and chamber humidity decreases, it is possible that certain ice nuclei are inhibited from reaching their activation thresholds. Hence, this factor as well as those proposed earlier (Mossop and Thorndike, 1966) may help explain the sample volume effect.

The independent and combined effects of various combinations of ice and condensation nuclei on the peak humidity are shown in Fig. 5. The ratio of IN to CCN determines the direction of a curve in the base plane as well as which type of nucleant is most important in restraining the humidity. Apart from the relative concentration of particles, the peak humidity will decrease for an increase in the concentration of either IN or CCN.

The possibility of increasing the humidity by operating the chamber with boundary values corresponding to no-sink humidities in excess of 100% was also investigated. Fig. 3d, which is a plot of the peak humidity against the calculated no-sink value, indicates that the peak humidity value can be increased but slight subsaturation is suggested even out to no-sink humidity values of 120%. Such large no-sink values required to approach water saturation may not be practical because condensation on the bottom of the chamber around the filter quite likely will add new sinks (ice) of vapor.

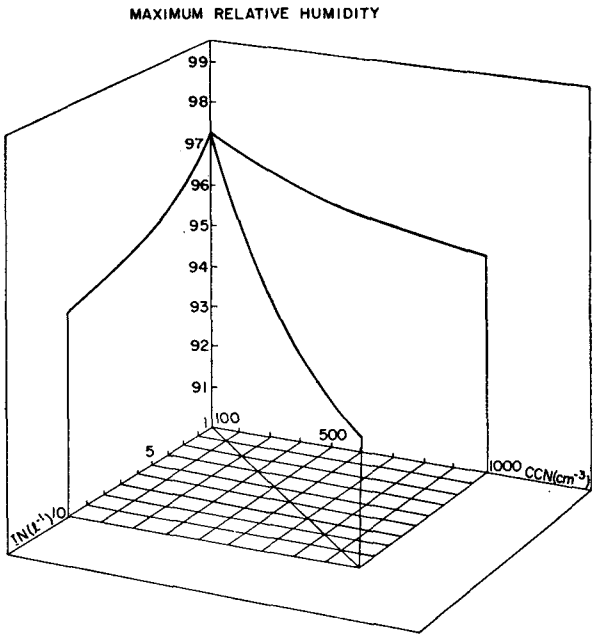

FIG. 5. Maximum relative humidity vs various concentrations of ice and cloud condensation nuclei.

Fig. 6a shows that larger time constants (slower cooling) lead to lower values of the peak humidity. This decrease in the peak humidity is the result of the difference of the time constants in the nucleation function and cooling function. Increasing the cooling time constant allows for the formation of a larger number of ice crystals before the filter temperature reaches its coldest steady-state value. The early formation of

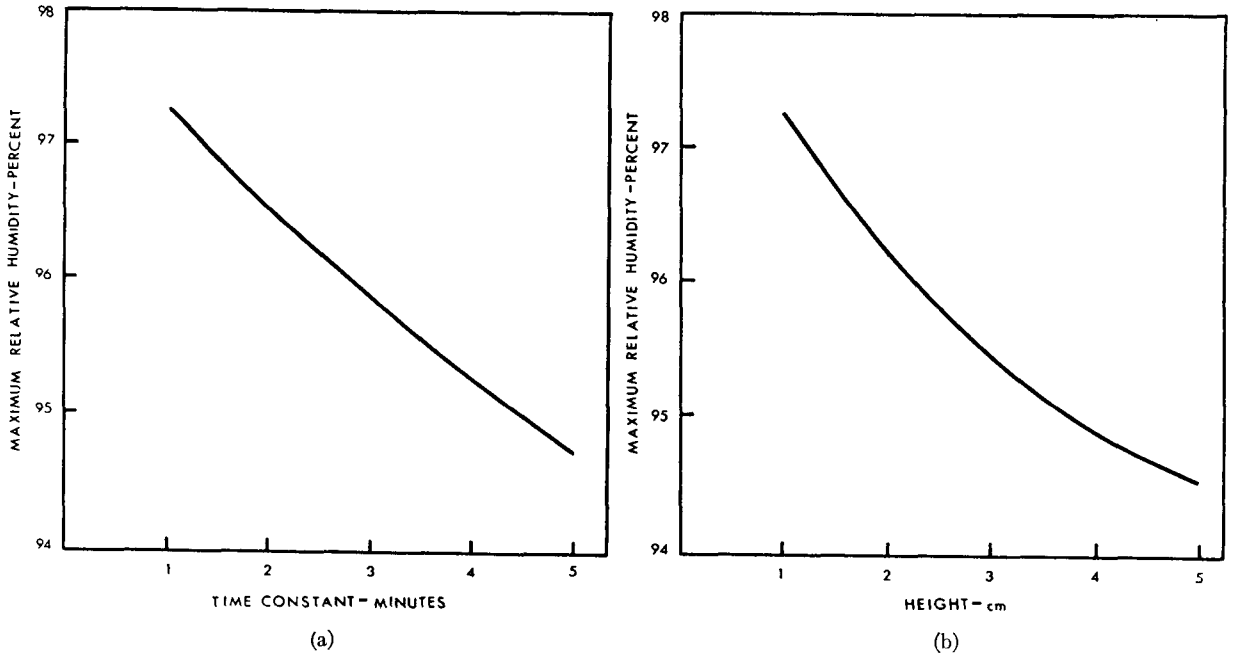

FIG. 6. Maximum filter relative humidity as a function of chamber cooling time constant (a) and height (b).

larger numbers of growing crystals during the slower cooling process retards the rise of the humidity.

The magnitude of the vapor flux from the upper surface is proportional to the height of the chamber. As evidenced in Fig. 6, the peak filter humidity falls with increasing chamber height. Again, the time-dependent humidity curves retain their shape (similar to Fig. 1 for 100 CCN cm^{-3}) but at lower values of humidity as the chamber height is increased. It might also be noted that the maximum humidity within the chamber occurs at the lower filter surface where temperatures are coldest. Obviously, chambers with minimum practical surface separations are to be preferred.

b. Interpretation of nucleus counts

If the physical framework and computations of this model are indeed representative of chamber conditions —and every attempt was directed toward this end— then we must reconsider the nature of ice-forming nuclei. The model indicates that, under a variety of practical operating conditions for the specified chamber geometry, water saturation is not likely to be reached at the surface of the filter. This subsaturated condition then excludes from consideration and measurement those nuclei requiring water saturation or slight supersaturation to become active.

There are, however, other possibilities for the explanation of the nucleus counts observed. The soluble nuclei present in the sample do form stable droplets at these subsaturated conditions and can freeze if during their growth they encounter an ice nucleus on the filter which initiates freezing by contact nucleation. Also, if the soluble nucleus also has an insoluble component capable of initiating freezing, an ice crystal can result from the drop. Deposition nuclei, nuclei which initiate ice crystals by the vapor-solid transition above ice saturation, constitute a third possibility.

Of the nucleation possibilities mentioned, perhaps the mixed nucleus concept is most tenable and common. It is becoming evident that most condensation nuclei consist of both a hygroscopic and non-hygroscopic component (Junge and McLaren, 1971). Hence, it would not be surprising if effective ice nuclei in the atmosphere, also subjected to agglomeration, gas adsorption and photochemical processes, possessed an analogous dual chemical composition.

Thus, several types of nuclei can account for the ice nucleus counts at slight subsaturated conditions. It appears thus far that the MF diffusion chamber technique cannot readily be used to distinguish these mechanisms from one another. The fact that these chambers might not quite achieve water saturation is not necessarily detrimental if the above types of nuclei are dominant in the atmosphere. Because there is a general comparability in IN data obtained with the MF technique and most other methods (Weickmann and Podzimek, 1971), the latter hypothesis is not unreasonable. However, more detailed data are needed, and the operating limits of any conditioning chamber should be clearly specified to facilitate nucleus interpretations and instrument comparisons.

4. Conclusions

The objective of this study was the formulation of a numerical model to simulate conditions in an ice nucleus chamber for conditioning millipore filters. Specifically, the aims were to examine (i) filter surface relative humidity for representative ice and condensation nucleus concentrations, (ii) particle activation and growth histories, (iii) the sample volume effect, and (iv) the effect of variations in the method of operating these chambers. The following conclusions emerged:

1) Water saturation with representative concentrations of nuclei and volumes equal to or greater than 100 $liter^{-1}$ is unlikely. Even with the chamber temperature differential set to give relative humidities in excess of 100% (with no sinks), the actual humidity is not likely to reach water saturation. After the humidity reaches its peak value, it then steadily declines as the ice crystals grow larger and become the dominant vapor sinks.

2) The maximum humidity decreases with an increasing number of sinks (nuclei of either type) on the filter. Thus, as the sample volume is increased and chamber humidity reduced, one might expect fewer ice nuclei to be activated. This seems to offer another possible explanation for the well-known volume effect.

3) Peak humidities are achieved in approximately 3–7 min depending on the cooling time constant in reaching the desired base temperature. Small time constants allow the humidity to reach higher values.

4) Assuming the model simulates actual conditions in the chambers in use, one must conclude that the nuclei are generally counted under slightly subsaturated (water) conditions and are either deposition (sublimation) nuclei, contact nuclei, or "mixed" condensation-freezing nuclei. Though by no means unequivocal, the latter type seems the most probable.

5) Mixed nuclei, i.e., a freezing nucleus containing a hygroscopic component that will allow some absorption of water at subsaturated humidities with subsequent freezing, may be fairly common.

6) These results suggest that chambers employing a flow of ice saturated air over a cooled filter may be more effective in approaching and maintaining water saturation for ice nucleus activation than methods relying solely on a diffusion process.

Acknowledgments. This research was supported by the National Science Foundation under Grant GA-12735 and by a Fellowship from the Office of the Chancellor of the State University of New York (Allocation 15-37-D).

APPENDIX A

List of Symbols

a	droplet curvature term
a_i	constant in Magnus equation for the ith phase
b	droplet solution term
b_i	constant in Magnus equation for the ith phase
C	ice crystal capacitance factor (cm)
D	diffusivity of water vapor in air ($cm^2\ sec^{-1}$)
e_0	vapor pressure of water at the triple point (dyn cm^{-2})
G, G'	thermodynamic factors for water and ice, respectively (Fletcher, 1966)
h	chamber height (cm)
i	index denoting water phase (1=water, 2=ice)
M	particle mass (gm)
N	number of crystals per unit area formed in a time t
N_0	number of ice nuclei per unit area
r	radius of drops (cm)
r_c	radius of crystals (cm)
S	ambient saturation ratio
S'	saturation ratio over a solution droplet ($1+a/r-b/r^3$)
t	time (sec)
t'	temperature (°C)
T	temperature (°K)
T_0, T_f	initial and final temperatures (°K)
z	distance (cm)
ρ	vapor concentration (gm cm^{-3})
ρ_{si}	saturation vapor concentration of ith phase
τ	time constant of cooling function
τ'	time constant of nucleation function
σ_{ij}	surface concentration of particles of the ith size class of the ith phase (cm^{-2})

APPENDIX B

Numerical Methods

The diffusion equation (1) was approximated by the difference equation

$$(1+\theta)\frac{\rho_j^{n+1}-\rho_j^{n}}{\Delta t}-\theta\frac{\rho_j^{n}-\rho_j^{n-1}}{\Delta t}=\frac{\rho_{j+1}^{n+1}-2\rho_j^{n+1}+\rho_{j-1}^{n+1}}{(\Delta z)^2},$$

where

$$\theta=\tfrac{1}{2}+\frac{(\Delta z)^2}{12D\Delta t}.$$

This equation is stable for all values of $D\Delta t/(\Delta z)^2$ and with θ as given produces a smaller error term (Richtmyer, 1967). The set of difference equations for the ρ_j^{n+1} were solved by Gauss elimination.

The droplet and crystal growth equations were solved with the predictor-corrector pair given by Hamming (1959):

$$\text{(predictor)}\quad r_{n+1}=r_{n-3}+4\Delta t(2\dot{r}_n-\dot{r}_{n-1}+2\dot{r}_{n-2})/3$$

$$\text{(corrector)}\quad r_{n+1}=[9r_n-r_{n-2}+3\Delta t\times(\dot{r}_{n+1}+2\dot{r}_n-\dot{r}_{n-1})]/8$$

Attempts to solve the corrector by iteration for the droplets were not successful because a small time step was required and the rate of convergence was slow. Better results were obtained by writing the corrector as a polynomial in the unknown r_{n+1} and solving for the roots. The root of interest was obtained by applying Newton's method in conjunction with a synthetic division algorithm. The initial approximation obtained from the predictor was always accurate enough to insure convergence to the proper root.

The complete set of equations consisting of the diffusion equation and equations for each class of droplets and crystals was solved at each time step. The predictor provided approximate values of radii which were used to produce an approximation to the vapor concentration. The vapor concentration value was then used with the corrector to produce better values of the radii. At this point a final value of vapor concentration was computed. This sequence of computations was sufficient (except for the first few time steps) to produce a relative error of less than 10^{-7}. In the early time steps one or two additional iterations were required to achieve this accuracy.

REFERENCES

Alkazweeny, A. J., 1970: The millipore technique for ice nuclei measurement. *J. Appl. Meteor.*, **9**, 796–799.

Bigg, E. K., S. C. Mossop, R. T. Mead and N. S. C. Thorndike, 1963: The measurement of ice nucleus concentrations by means of millipore filter. *J. Appl. Meteor.*, **2**, 266–269.

——, and C. M. Stevenson, 1970: Comparison of ice nuclei in different parts of the world. *J. Rech. Atmos.*, **4**, 41–58.

Fletcher, N. H., 1959: On ice crystal production by aerosol particles. *J. Meteor.*, **2**, 173–180.

——, 1966: *The Physics of Rainclouds*. Cambridge University Press, 390 pp.

Gagin, A., and M. Aroyo, 1969: A thermal diffusion chamber for the measurement of ice nucleus concentrations. *J. Rech. Atmos.*, **4**, 115–122.

Hamming, R. W., 1959: Stable predictor-corrector methods for ordinary differential equations. *J. Assoc. Comput. Mach.*, **6**, 37–47.

Jiusto, J., D. A. Paine and M. L. Kaplan, 1970: Great Lakes snowstorms (Part 2). NOAA Grant E22-13-69G, ASRC, State University of New York, Albany, p. 35.

Junge, C., and E. McLaren, 1971: Relationship of cloud nuclei spectra to aerosol size distribution and composition. *J. Atmos. Sci.*, **28**, 382–390.

Mossop, S. C., and N. S. C. Thorndike, 1966: The use of membrane filters in measurements of ice nucleus concentration. I. Effect of sampled air volume. *J. Appl. Meteor.*, **5**, 474–480.

Nakaya, A., 1954: *Snow Crystals, Natural and Artificial*. Harvard University Press, 510 pp.

Richtmyer, R. D., 1967: *Difference Methods for Initial Value Problems*. New York, Interscience, 405 pp.

Stevenson, C. M., 1968: An improved millipore filter technique for measuring the concentration of freezing nuclei in the atmosphere. *Quart. J. Roy. Meteor. Soc.*, **94**, 35–43.

Twomey, S., 1959: The nuclei of natural cloud formation—Part I. *Geof. Pura, Appl.* **43**, 227–242.

Weickmann, H. K., and J. Podzimek, 1971: *Second Intern. Workshop Condensation and Ice Nuclei*, IUGG Congress, Moscow. (See *Workshop Proc.*, 1971: L. O. Grant, ed., Colorado State Univ.).